

Research Paper

Cite this article: Arnaud E, Huitema L, Chantalat R, Bellion A, Monediere T (2019). Circularly polarized ferrite patch antenna for LEO satellite applications. *International Journal of Microwave and Wireless Technologies* 1–7. <https://doi.org/10.1017/S1759078719001429>

Received: 2 May 2019

Revised: 27 September 2019

Accepted: 4 October 2019

Key words:

Circularly polarized patch antenna; ferrite substrate; space applications

Author for correspondence:

E. Arnaud, E-mail: eric.arnaud@xlim.fr

Circularly polarized ferrite patch antenna for LEO satellite applications

E. Arnaud¹ , L. Huitema¹, R. Chantalat², A. Bellion³ and T. Monediere¹

¹XLIM – CNRS, 123 Avenue Albert Thomas, 87060 Limoges Cedex, France; ²CISTEME, 12 rue Gémini 87069 Limoges Cedex, France and ³CNES, 18 avenue Edouard Belin, 31401 – Toulouse, France

Abstract

This paper presents the capacity of an S band circularly polarized patch antenna using a ferrite material for low-earth orbiting satellites (2025–2100 MHz for TeleCommand) to obtain a semi-isotropic radiation pattern. Indeed, circularly polarized antennas are generally large and bulky which is often incompatible for spatial applications especially for small satellites. A new antenna design is proposed with the following maximum dimensions: a diameter of 80 mm and a height of 12 mm. The structure presents an axial ratio lower than 6 dB (according to requirements) and a realized gain higher than -6 dB over a 4% bandwidth at the limit of coverage i.e. 90° irrespective of the azimuth angle (φ).

Introduction

Nowadays, the circular polarization purity of control link antennas for low earth orbiting (LEO) satellites is essential. Indeed, this purity directly impacts the gain, the overall satellite link quality (phenomena of atmospheric depolarization), and it also increases the data rate in the case of dual circular polarization. Circularly polarized antennas are often difficult to develop. The limit of coverage (LOC) for which the axial ratio (AR) is lower than 6 dB and the associated bandwidth is often narrow. Furthermore, many space applications, especially nanosatellites, require planar antennas and/or compact antennas. These antennas can be:

- a microstrip patch antenna with two stubs, two notches or a diagonal slot. These antennas suffer from a narrow bandwidth [1 (https://cdn4.endurosat.com/modules-datasheets/S-Band_Patch_User_Manual_Rev1_2.pdf <https://www.endurosat.com/products/cubesat-s-band-patch-antenna>)]
- a dual-fed patch antenna with two offset lines or a 3 dB 90° hybrid coupler [1]. The first one also suffers from a narrow bandwidth while the second is more complex to develop and often less compact.

It is therefore important to look for alternatives to these solutions in order to simplify and “naturally” generate right and left handed circular polarizations (RHCP and LHCP) on both a wide bandwidth and angular coverage. The aim of this study is to explore the potentiality of microstrip ferrite antennas to meet this challenge. The aim here is to use the natural ability of polarized ferrites to generate circularly polarized waves on S-band frequencies of satellite missions (2025–2100 MHz for TeleCommand) and to obtain a semi-isotropic radiation pattern. The expected performances, provided by the French Spatial Agency, are presented in Table 1.

The first ferrite antenna was designed in 1956 by D. J. Angelakos team by inserting a ferrite block at the output of a waveguide [2]. A beam steering, depending on the ferrite thickness and the applied direct current (DC) magnetic bias field, was obtained. In [3, 4], the authors showed that it is possible to obtain a more compact microstrip antenna by using a ferrite substrate rather than a purely dielectric one. Moreover, bandwidth and efficiency are higher. In 1992, Roy *et al.*, designed a circularly polarized microstrip antenna using an axially polarized ferrite substrate [5]. The same year, D. Pozar presented an analytical method (based on a cavity model) to better understand how these circularly polarized antennas work [6]. He also showed that the magnetized ferrite substrate produced switchable and tunable circularly polarized radiation. In [7, 8], a ring microstrip antenna on a biased ferrite substrate was presented. Firstly, the feed was a coaxial probe. Due to the difficulty of drilling a hole in ferrite, the use of an electromagnetically coupled feed was then studied. Since 2009, Zervos *et al.*, have studied these antennas by comparing the results of several configurations (influence of the ferrite substrate size, feeding technique, etc.) [9, 10]. All these antenna designs were realized with a magnet placed behind the ground plane in order to polarize the ferrite. This is incompatible with the antenna compactness. Here, a solution is proposed to minimize the height. A magnetostatic study is also carried out to correctly model the ferrite characteristics and the antenna behavior. The paper is organized as follows. “General properties of ferrites and comparison

Table 1. Antenna performance target

Parameter	Specification
Frequency band (GHz)	2.025–2.11 (4%)
Return loss (dB)	<−15
Polarization	RHCP or LHCP
LOC	90°
Minimum gain at LOC (dB)	−6.0
Maximum AR (dB) at LOC	6.0
Total losses (dB)	0.5
Maximum antenna dimensions	80 mm of diameter and 12 mm of height

between an ideal and a real magnetization” reminds the general properties of ferrites and compares (at 2 GHz) the performances of a ferrite antenna when it is ideally polarized (theoretical case) and when it is magnetized with a real permanent magnet. “Antenna description” describes the final design taking into account the dimensional constraints to achieve the desired antenna characteristics over the entire frequency band. The comparison between simulations and measurements is presented in “Measurement and simulation”. Finally, a conclusion is given.

General properties of ferrites and comparison between an ideal and a real magnetization

General properties of ferrites

The ferrite material generates “naturally” a circular polarization when it is biased by a DC magnetic field H_0 . In [5], the authors presented how to take advantage of the non-reciprocity properties of ferrites by obtaining a circular polarized patch antenna. This non-reciprocity *phenomenon of a ferrite material is described by its permeability tensor. For a biasing DC magnetic field applied along the z axis and sufficient to saturate the ferrite, this permeability tensor is given by equation (1) [11].*

$$\mu = \mu_0 \overline{\overline{\mu_r}} = \mu_0 \begin{bmatrix} \mu_1 & -j\mu_2 & 0 \\ j\mu_2 & \mu_1 & 0 \\ 0 & 0 & 1 \end{bmatrix} \quad (1)$$

where

$$\mu_1 = 1 + \frac{\omega_m \omega_0}{\omega_0^2 - \omega^2}, \quad \mu_2 = \frac{\omega_m \omega}{\omega_0^2 - \omega^2}, \quad \omega_0 = \gamma \mu_0 H_i + j\omega\alpha,$$

$$\omega_m = \gamma \cdot \mu_0 \cdot 4 \pi M_s$$

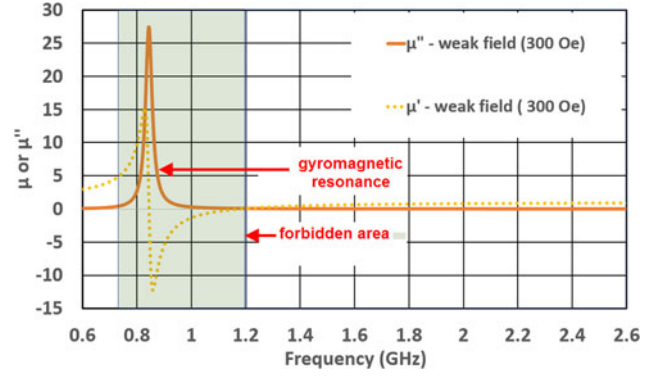
γ is the gyromagnetic ratio and α is the damping factor

$$\gamma = 1.4 G_{eff}$$

where G_{eff} is the effective Landé factor, H_i internal magnetic field

$$\alpha = \frac{\gamma \cdot \Delta H}{2 \cdot \omega}$$

where ΔH is the resonance line width (close to the resonant frequency)

**Fig. 1.** Evolution of the real and imaginary parts of μ_1 according to frequency and the Polder tensor.

Therefore, both μ_1 and μ_2 are depending on the internal DC magnetic field in the ferrite material H_i , the saturation magnetization M_s , and the frequency f . When both the real and the imaginary parts of μ_1 , i.e. μ_1' and μ_1'' respectively, are drawn, a resonance called gyromagnetic resonance (f_r) appears: $f_r = \gamma H_i = 1.4 G_{eff} H_i$ with G_{eff} in (MHz/Oe).

Around this resonance frequency, the magnetic losses (proportional to μ_1'') are too high and for frequencies just above the gyromagnetic resonance, the effective permeability of ferrite which is defined as $\mu_{eff} = (\mu_1'^2 - \mu_2'^2) / \mu_1'$ becomes negative. Thus, Pozar has shown that the ferrite material was not usable on these frequency bands. These areas are illustrated in Fig. 1 and explained in [12].

For this study, the antenna works above the gyromagnetic resonance (weak field). The ferrite used is therefore Y36 ferrite (Table 2) with a low-saturation magnetization ($4 \pi M_s = 290$ Gauss) which allows the use of a less powerful and bulky permanent magnet to obtain the material saturation. Furthermore far from resonance, the Y36 ferrite has a small effective resonance line width ΔH_{eff} (Oe), minimizing magnetic losses. With the Y36 ferrite characteristics, the real and the imaginary parts of μ_1 , i.e. μ_1' and μ_1'' are plotted in Fig. 1 for a uniform H_i in the ferrite material equal to 300 Oe. This graph shows the operating and forbidden areas.

Study of principle

Before designing an antenna that best meets the requirements, a first magnetostatic and electromagnetic co-simulation has been carried out on a simple case using CST Microwave Studio to show the importance of the H_i uniformity in the ferrite. A

Table 2. Y36 ferrite characteristics (<http://www.exxelia.com/fr/groupe/a-propos/temex>)

Parameter	Specification
Saturation magnetization $4 \pi M_s$ (Gauss)	290
Effective resonance line width ΔH_{eff} (Oe)	4
Resonance line width ΔH (Oe)	25
Relative permittivity (ϵ_r)	13.7
Loss tangent ($\tan \delta$)	0.0002
Effective Landé factor (G_{eff})	2.01

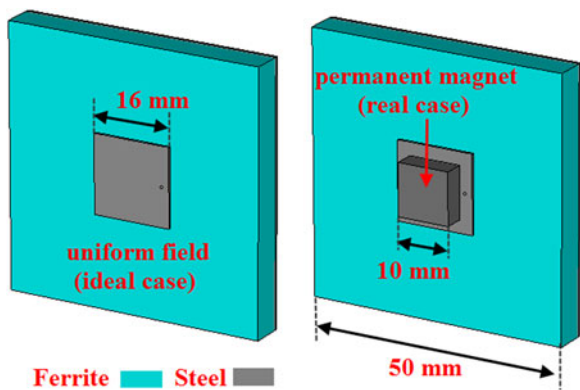


Fig. 2. Test patch antenna.

patch antenna presented in Fig. 2 has been therefore simulated to compare the ideal and real magnetization. Initially, the ferrite is submitted to an ideal and uniform H_i field of 300 Oe. This case is called “ideal case”. Then, a well-chosen 4 mm thickness permanent magnet is placed over the antenna top hat in order to create an internal static magnetic field close to 300 Oe in the material. This case is called “real case”. The simulation is made using the magnetostatic and electromagnetic modules of CST Microwave Studio. Figure 3 shows that it is possible to obtain the same boresight AR between the ideal and real case by taking a remanent flux density (Br) of 0.7 T for the magnet.

For this configuration, magnetic and dielectric losses are high (Fig. 4). This can be explained by looking at H_i in Fig. 5(a). It appears that for $Br = 0.7$ T, the DC magnetic field is sometimes close to 700 Oe. Thus, for a working frequency of 2 GHz we are close to the high-loss gyroresonance area ($f_r = 700$ Oe. 2.8 MHz/Oe = 1.96 GHz). It is necessary to change the magnet (reduce the Br to 0.4 T) to have reasonable losses. In this case, we can see that the AR is increased and the bandwidth is reduced which is due to the presence of a non-uniform H_i in the ferrite (Fig. 5(b)). There is a trade-off between circular polarization performances, impedance bandwidth, and the antenna losses. In our study, the minimization of these last ones was the most important.

Antenna description

After a reminder of ferrite properties and an explanation of the importance of H_i , this section describes the final design taking into account the previous conclusion and the dimensional

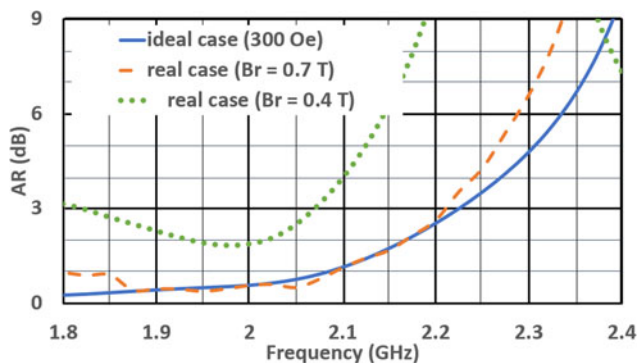


Fig. 3. Comparison of the boresight AR (ideal and real cases).

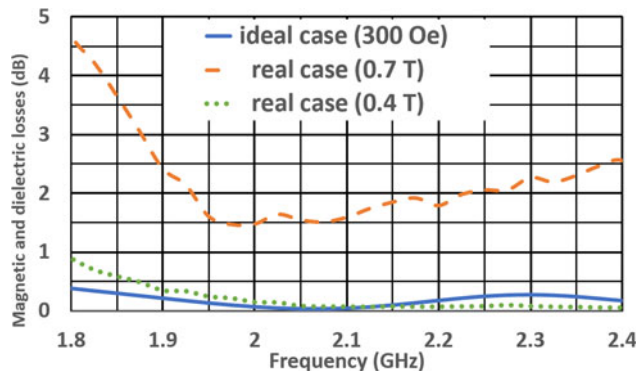


Fig. 4. Comparison of the magnetic and dielectric losses (ideal and real cases).

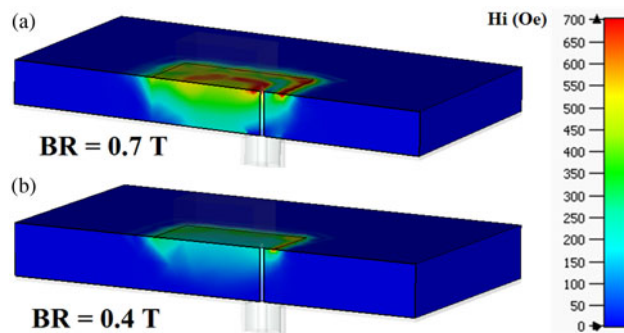


Fig. 5. DC internal magnetic bias field within the ferrite (H_i).

constraints to achieve the desired antenna characteristics. The design presented in Fig. 2 is not suitable for the requirements due to its narrow impedance matching bandwidth. To improve this characteristic, the antenna is modified. The radiating part of the new structure consists of two stacked patches ($\phi_{patch1} = 12.4$ mm and $\phi_{patch2} = 24$ mm) glued on a 4.98 mm thickness polyetheretherketone plastic (PEEK, $\epsilon_r = 3.1$ and $\tan\delta = 0.004$). This new choice for the radiating part and the dimensions of the antenna (12 mm height and 80 mm diameter) requires changing the position and shape of the permanent magnet. Finally, Fig. 6 shows the new design. To our knowledge, no one has made a patch antenna using a ferrite material without a permanent magnet behind the ground plane. The magnetization around the ferrite is therefore innovative. The feeding part of this patch antenna is obtained using a microstrip-slot transition. A slot ($L_{slot} = 25$ mm) and a microstrip line is machined respectively on a 0.5 mm E24 steel disc and etched on the bottom of a 0.508 mm thickness laminate Duroid RT5870. The top the aforementioned substrate is completely etched. E24 disc corresponds to the patch antenna ground plane (GND). As it is made of steel, it also improves the H_i distribution inside the 6 mm thickness ferrite disc (40 mm of diameter) placed above and in the middle of the GND. A SMP-M type coaxial connector is soldered to the input of the microstrip line. A 6 mm thick ring-shaped neodymium permanent magnet with a negative axial direction of magnetization surrounds the Y36 ferrite. With this orientation, the antenna produces a LHCP. The inner and outer diameters are respectively 60 and 70 mm and the remanent field Br of the permanent magnet is 1.22 T. These parameters have been optimized to avoid the H_i inside the ferrite close to 700 Oe. A 0.5 mm E24 washer is located on the top of the magnet to improve H_i . The support is

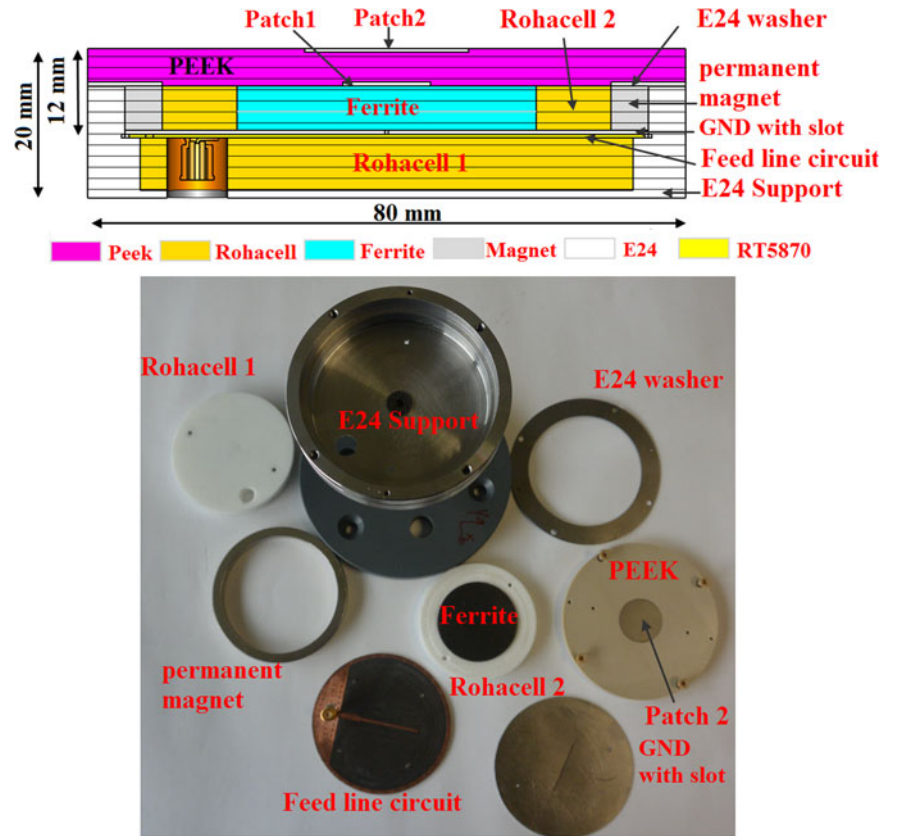


Fig. 6. Cut-plane view and the exploded antenna photograph.

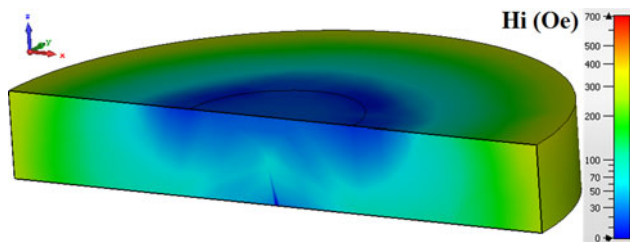


Fig. 7. DC internal magnetic bias field within the ferrite (H_i).

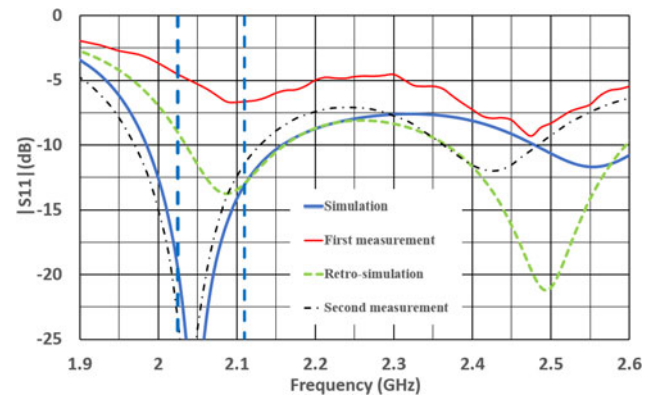


Fig. 9. Simulated and measured S_{11} parameter.

also made of steel for the same reasons. This last one also creates a cylindrical cavity below the patch feed and reduces the antenna back radiation due to the slot.

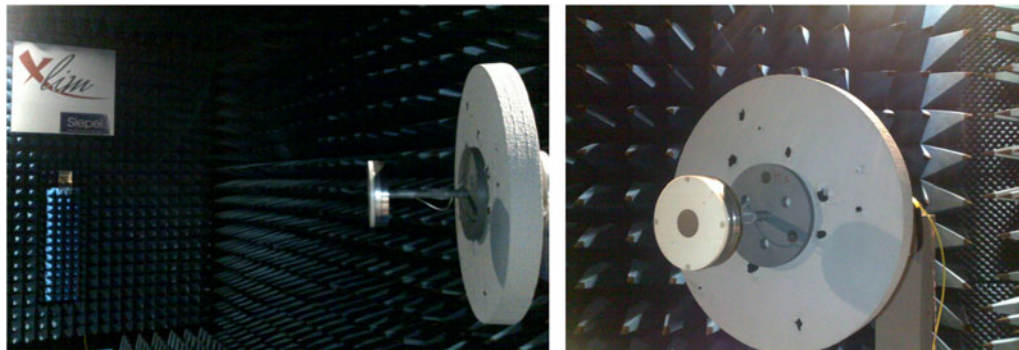


Fig. 8. Photograph of the antenna positioned on our ATRS.

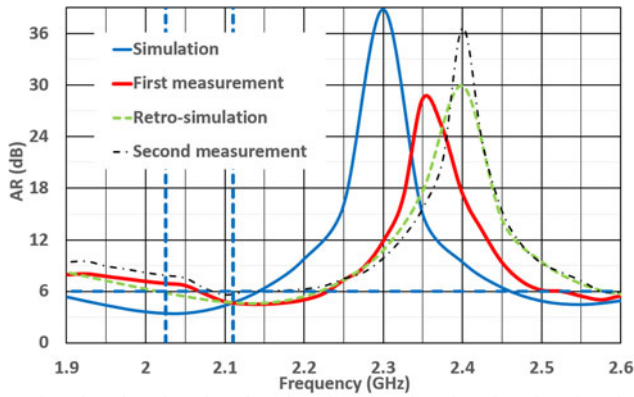


Fig. 10. Simulated and measured AR.

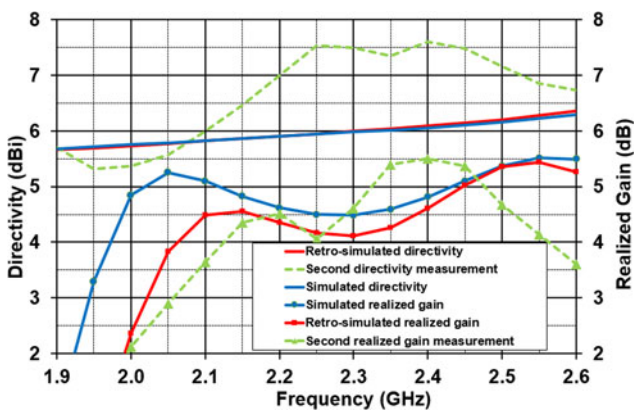


Fig. 11. Simulations and measurements of the boresight directivity and RG.

Measurement and simulation

A new magnetostatic and electromagnetic co-simulation was done. Figure 7 presents the “real” internal magnetic field H_i within the realized antenna. It is, as desired, well below

700 Oe with a 150 Oe average value. Figure 8 shows a photograph of the antenna positioned on our antenna test range support (ATRS). The first measurement shows measured S_{11} parameter which is quite different from the simulation (Fig. 9). In simulation, the impedance bandwidth is greater than 8%. A frequency shift appears, the antenna operates at higher frequencies and the level is also higher. Simulations have been done to explain these differences and the best explanation remains the decrease of the ferrite relative permittivity ($\epsilon_r = 11.0$ instead 13.7). With this value, to meet the desired characteristics, notably the amplitude of the S_{11} parameter, the slot length also had to be increased in simulation and in realization. Taking into account these two changes, a new simulation called “retro-simulation” has been realized. Figure 9 shows the retro-simulation and the new measurement after this change (second measurement). Even if the measurement result is not identical to the theory, the antenna now has a good impedance matching. Figure 10 compares the boresight AR in different cases. Initially, it is lower than 6 dB in the frequency bandwidth (12%). With the kind of antenna, the AR bandwidth is generally greater than the impedance bandwidth. Unfortunately, the mistake of the ferrite relative permittivity value increases the AR level and decrease the bandwidth.

The directivity and realized gain (RG) are plotted in Fig. 11. Initially, the simulated directivity and RG were similar, so total losses were close to 0.5 dB in bandwidth. The measured directivity is like the simulated one even if the radiation patterns are disturbed by the ATRS. After all the changes, the simulated total losses are increased (2 dB). This is due to metal losses induced by the steel on the ground plane. The electromagnetic field distribution is different for each case. For the last case, this field is higher and so causes more losses. The measured total losses are also increased (<3 dB). The three-dimensional (3D) LHCP radiation pattern theory-measurement comparison (Fig. 12) is presented at 2.1 GHz in directivity after the modifications. Figure 13(a)–(d) compare the simulated and measured LHCP RG and AR at 2.1 GHz. The result is almost identical to the other frequencies. The minimum gain in LOC is greater than -6 dB in simulation and measurement even if the radiation patterns of the latter are less symmetrical. It is not possible at this

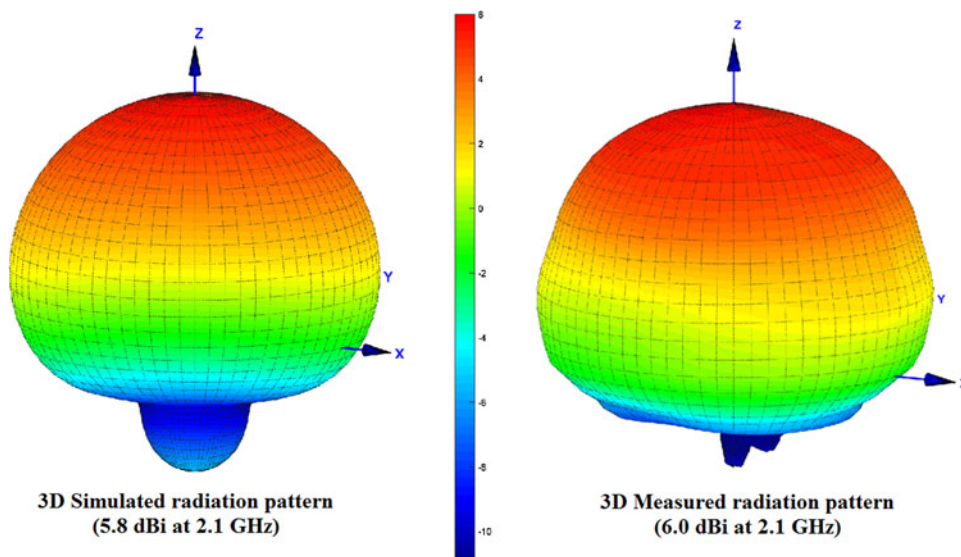


Fig. 12. 3D radiation patterns.

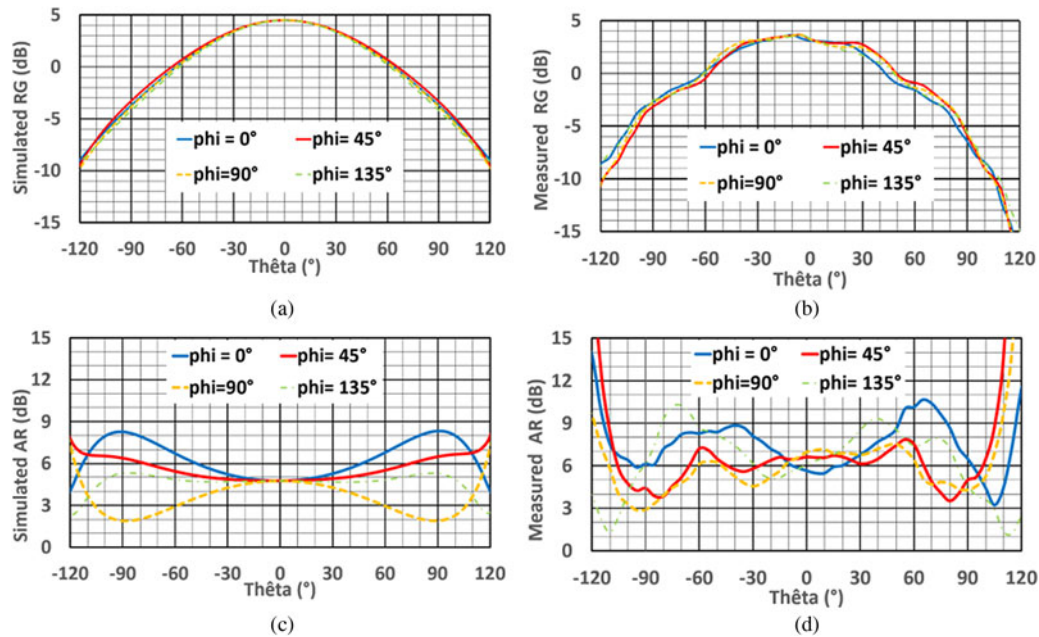


Fig. 13. Radiation patterns (2.1 GHz). (a) LHCP simulated RG. (b) LHCP measured RG. (c) Simulated AR. (d) Measured AR.

time to have an AR in LOC lower than 6 dB even in the simulation. It would take a boresight AR close to 3 dB to have a good AR in the LOC. This condition is perhaps possible but it would be necessary to perfectly know all the parameters of the antenna, notably the ferrite permittivity at the working frequency. Then, it would be necessary to redesign the antenna, in particular ferrite and permanent magnet dimensions taking into account these new parameters.

Conclusion

This paper studies the ability of a ferrite patch antenna to obtain S band circularly polarized radiation for LEO satellites. It meets the requirements in simulation in terms of circular polarization, compactness, and ease of manufacturing. After changing the ferrite relative permittivity value, a good agreement between retro-simulation and measurement has been obtained. This kind of antenna is therefore likely to meet the requirements of LEO satellites.

Acknowledgement. The authors would like to thank French Space Agency – CNES (Centre National d'Etudes Spatiales) – FRANCE who has financially supported this study.

References

1. Carver K and Mink J (1981) Microstrip antenna technology. *IEEE Transactions on Antennas and Propagation* **29**, 2–24.
2. Angelakos DJ and Korman MM (1956) Radiation from ferrite-filled apertures. *Proceedings of the IRE* **44**, 1463–1468.
3. Das N and Chowdhury SK (1980) Microstrip rectangular resonators on ferrimagnetic substrates. *Electronics Letters* **16**, 817–818.
4. Das N, Chowdhury S and Chatterjee J (1983) Circular microstrip antenna on ferrimagnetic substrate. *IEEE Transactions on Antennas and Propagation* **31**, 188–190.
5. Roy JS, Vaudon P, Reineix A, Jecko F and Jecko B (1992) Axially magnetized circular ferrite microstrip antenna. *IEEE Antennas and Propagation Society International Symposium 1992 Digest*, Chicago, IL, USA, vol.4, pp. 2212–2215, doi: 10.1109/APS.1992.221425.

6. Pozar DM (1992) Radiation and scattering characteristics of microstrip antennas on normally biased ferrite substrates. *IEEE Transactions on Antennas and Propagation* **40**, 1084–1092.
7. Tsang KK and Langley RJ (1994) Annular ring microstrip antennas on biased ferrite substrates. *Electronics Letters* **30**, 1257–1258.
8. Tsang KK and Langley RJ (1998) Design of circular patch antennas on ferrite substrates. *IEE Proceedings – Microwaves, Antennas and Propagation* **145**, 49–55.
9. Zervos T, Alexandridis DAA, Lazarakis F, Pissas M, Stamopoulos D, Angelopoulos ES and Dangakis K (2012) Design of a polarisation reconfigurable patch antenna using ferrimagnetic materials. *IET Microwaves, Antennas & Propagation* **6**(2), 158–164. doi: 10.1049/iet-map.2011.0224
10. Andreou E, Zervos T, Lazarakis F, Alexandridis AA, Dangakis K, Varouti E, Fikioris G and Vardaxoglou JC (2014) Reconfigurable proximity coupled patch antenna using magnetic bias. *2014 Loughborough Antennas and Propagation Conference (LAPC)*, Loughborough, pp. 376–380. doi: 10.1109/LAPC.2014.6996401.
11. Polder D (1949) VIII. On the theory of ferromagnetic resonance, The London, Edinburgh, and Dublin philosophical magazine. *Journal of Science* **40**, 99–115.
12. Arnaud E, Huitema L, Chantalat R, Bellion A and Monédière T (2018) Miniaturization of a circular polarized antenna using ferrite materials. *12th European Conference on Antennas and Propagation (EUCAP)*, April 2018, London, UK.



Eric Arnaud was born in France in 1970. He received the Diplôme D'Etudes Supérieures Spécialisées (DESS) and Ph.D. degrees in Electronics and Telecommunication from the University of LIMOGES in 1994 and 2010, respectively. He did his Ph.D. on circularly polarized EBG antenna. From 1996 to 2001, he has been in charge of the Microwave part of Free-Electron Laser (L.U.R.E). Since 2001, he has been in charge of XLIM laboratory's antenna test range. He participated in several research projects related to the design, development, and characterization of antennas. His research interests are mainly in the fields of circularly polarized EBG antenna, agile electromagnetic band gap matrix antenna, and isoflux pattern antenna.



Laure Huitema received the M.S. and Ph.D. degrees in telecommunications high frequencies and optics from Limoges University, in 2008 and 2011, respectively. From 2011 to 2012, she was a Postdoctoral Research Fellow at the Atomic Energy Commission (CEA), Laboratory of Electronics and Information Technology (LETI), Grenoble, France. Currently, she is an Associate Professor in the antennas and signals

team within the RF system axis of the XLIM Research Institute, University of Limoges, France. Her research interests include reconfigurable antennas, dielectric resonator antennas, miniature antennas, and multiband antennas. More recently, she has been working on new components for their integration inside antennas. In this framework, she is the Project Leader of a H2020 European project called MASTERS (http://www.unilim.fr/H2020_MASTERS/). Dr. Huitema was the recipient of the Best Student Paper award at the 2010 IEEE International Workshop on Antenna Technology and of the Best Student Paper Award at the 2010 JCMM Conference.



Régis Chantalat was born in Brive La Gaillarde, France, in 1976. He received the Ph.D. degrees in telecommunications high frequencies and optics from Limoges University, Limoges, in 2003. He is currently the RF Component Team Manager of the Center for Innovation and Technology Transfer CISTEME (Center for Engineering of Telecommunications Systems in ElectroMagnetism and Electronics),

Limoges, France. His current research interests include design of RF chain components (active and passive), reflector and lens antennas, horns antennas,

helicoidal antennas, miniature and integrated antennas, antennas array, high power antennas, periodic structure antennas, multiband antennas, UWB antennas, and monopolar antennas.



Anthony Bellion received his Engineer Diploma in Electronics in 2003 from the Ecole Nationale Supérieure d'Ingénieurs de Limoges (ENSIL) (Limoges, France). He received his Ph.D. degree in optical communication and microwave techniques from the University of Limoges, Limoges, France in 2008 working on Multi polarizations & UWB antenna designs for direction finding systems. After industrial

experience with Thales, France, he joined the Antenna Department of the French Space Agency (CNES). Since 2016, he has headed the CNES Antenna Department. His areas of research are mainly UWB antennas, miniature antennas design, and characterization.



Thierry Monediere was born in 1964 in Tulle (France). He obtained his Ph.D. in 1990 in the IRCOM Laboratory of the University of Limoges. He is actually a Professor in the "Antennas and signals" team of the Xlim research Laboratory in the University of Limoges. He develops his research activities in this Lab and works on multifunction antennas, miniature antennas, antenna arrays, and also

active antennas. He also studies gyromagnetic devices as ferrite circulators or isolators.